

# Integrating Behavior Cloning and Reinforcement Learning for Improved Performance in Sparse Reward Environments

Vinicius G. Goecks,<sup>1,2</sup> Gregory M. Gremillion,<sup>1</sup> Vernon J. Lawhern,<sup>1</sup>

John Valasek,<sup>2</sup> Nicholas R. Waytowich<sup>1,3</sup>

<sup>1</sup>US Army Research Laboratory, <sup>2</sup>Texas A&M University, <sup>3</sup>Columbia University  
vinicius.goecks@tamu.edu, {gregory.m.gremillion, vernon.j.lawhern}.civ@mail.mil,  
valasek@tamu.edu, nicholas.r.waytowich.civ@mail.mil

## Abstract

This paper investigates how to efficiently transition and update policies, trained initially with demonstrations, using off-policy actor-critic reinforcement learning. It is well-known that techniques based on Learning from Demonstrations, for example behavior cloning, can lead to proficient policies given limited data. However, it is currently unclear how to efficiently update that policy using reinforcement learning as these approaches are inherently optimizing different objective functions. Previous works have used loss functions which combine behavioral cloning losses with reinforcement learning losses to enable this update, however, the components of these loss functions are often set anecdotally, and their individual contributions are not well understood. In this work we propose the Cycle-of-Learning (CoL) framework that uses an actor-critic architecture with a loss function that combines behavior cloning and 1-step Q-learning losses with an off-policy pre-training step from human demonstrations. This enables transition from behavior cloning to reinforcement learning without performance degradation and improves reinforcement learning in terms of overall performance and training time. Additionally, we carefully study the composition of these combined losses and their impact on overall policy learning. We show that our approach outperforms state-of-the-art techniques for combining behavior cloning and reinforcement learning for both dense and sparse reward scenarios. Our results also suggest that directly including the behavior cloning loss on demonstration data helps to ensure stable learning and ground future policy updates.

## Introduction

Reinforcement Learning (RL) has yielded many recent successes in solving complex tasks that meet and exceed the capabilities of human counterparts, demonstrated in video game environments (Mnih et al. 2015), robotic manipulators (Andrychowicz et al. 2018), and various open-source simulated scenarios (Lillicrap et al. 2015). However, these RL approaches are sample inefficient and slow to converge to this impressive behavior, limited significantly by the need

to explore potential strategies through trial and error, which produces initial performance significantly worse than human counterparts. The resultant behavior that is initially random and slow to reach proficiency is poorly suited to various situations, such as physically embodied ground and air vehicles or in scenarios where sufficient capability must be achieved in short time spans. In such situations, the random exploration of the state space of an untrained agent can result in unsafe behaviors and catastrophic failure of a physical system, potentially resulting in unacceptable damage or downtime. Similarly, slow convergence of the agent's performance requires exceedingly many interactions with the environment, which is often prohibitively difficult or infeasible for physical systems that are subject to energy constraints, component failures, and operation in dynamic or adverse environments. These sample efficiency pitfalls of RL are exacerbated even further when trying to learn in the presence of sparse reward, often leading to cases where RL can fail to learn entirely.

One approach for overcoming these limitations is to utilize demonstrations of desired behavior from a human data source (or potentially some other agent) to initialize the learning agent to a significantly higher level of performance than is yielded by a randomly initialized agent. This is often termed learning from demonstrations (LfD) (Argall et al. 2009), which is a subset of imitation learning that seeks to train a policy to imitate the desired behavior of another policy or agent. LfD leverages data (in the form of state-action tuples) collected from a demonstrator for supervised learning, and can be used to produce an agent with qualitatively similar behavior in a relatively short training time and with limited data. This type of LfD, called Behavior Cloning (BC), learns a mapping between the state-action pairs contained in the set of demonstrations to mimic the behavior of the demonstrator.

Though BC techniques do allow for the relatively rapid learning of behaviors that are comparable to that of the demonstrator, it is limited by the quality and quantity of the demonstrations provided and is only improved by providing additional, high-quality demonstrations. In addition, BC is plagued by the distributional drift problem in which a mismatch between the learned policy distribution of states and

the distribution of states in the training set can cause errors that propagate over time and lead to catastrophic failures. By combining BC with subsequent RL, it is possible to address the drawbacks of either approach, initializing a significantly more capable and safer agent than with random initialization, while also allowing for further self-improvement without needing to collect additional data from a human demonstrator. However, it is currently unclear how to effectively update a policy initially trained with BC using reinforcement learning as these approaches are inherently optimizing different objective functions. Previous works have used loss functions that combine BC losses with RL losses to enable this update, however, the components of these loss functions are often set anecdotally and their individual contributions are not well understood.

In this work, we propose the Cycle-of-Learning (CoL) framework, which uses an actor-critic architecture with a loss function that combines behavior cloning and 1-step Q-learning losses with an off-policy, pre-training step from human demonstrations. The main contribution of this work is a method to enable transition from behavior cloning to reinforcement learning without performance degradation while improving reinforcement learning in terms of overall performance and training time. Additionally, we examine the effect of these combined losses on overall policy learning in two continuous action space environments. Our results show that our approach outperforms BC, Deep Deterministic Policy Gradients (DDPG), and DDPG from Demonstrations (DDPGfD) in two different application domains for both dense and sparse reward settings. We show that our CoL method was the only method to produce a viable policy for one of the two environments designed specifically to exhibit a high degree of stochasticity. In addition, we show that in dense-reward settings the performance of DDPGfD suffers significantly due to its inclusion of  $n$ -step Q-learning loss. Our results also suggest that directly including the behavior cloning loss on demonstration data helps to ensure stable learning and ground future policy updates, and that a pre-training step enables the policy to start at a performance level greater than behavior cloning.

## Preliminaries

We adopt the standard Markov Decision Process (MDP) formulation for sequential decision making (Sutton and Barto 1998), which is defined as a tuple  $(S, A, R, P, \gamma)$ , where  $S$  is the set of states,  $A$  is the set of actions,  $R(s, a)$  is the reward function,  $P(s'|s, a)$  is the transition probability function and  $\gamma$  is a discount factor. At each state  $s \in S$ , the agent takes an action  $a \in A$ , receives a reward  $R(s, a)$  and arrives at state  $s'$  as determined by  $P(s'|s, a)$ . The goal is to learn a behavior policy  $\pi$  which maximizes the expected discounted total reward. This is formalized by the Q-function, sometimes referred to as the state-action value function:

$$Q^\pi(s, a) = \mathbb{E}^\pi \left[ \sum_{t=0}^{+\infty} \gamma^t R(s_t, a_t) \right]$$

taking the expectation over trajectories obtained by executing the policy  $\pi$  starting at  $s_0 = s$  and  $a_0 = a$ .

Here we focus on actor-critic methods which seek to maximize

$$J(\theta) = \mathbb{E}_{s \sim \mu} [Q^{\pi(\cdot|\theta)}(s, \pi(s|\theta))]$$

with respect to parameters  $\theta$  and an initial state distribution  $\mu$ . The Deep Deterministic Policy Gradient (DDPG) (Lillicrap et al. 2015) is an off-policy actor-critic reinforcement learning algorithm for continuous action spaces, which calculates the gradient of the Q function with respect to the action to train the policy. DDPG makes use of a replay buffer to store past state-action transitions and target networks to stabilize Q-learning (Mnih et al. 2015). Since DDPG is an off-policy algorithm, it allows for the use of arbitrary data, such as demonstrations, to update the policy. A demonstration trajectory is a tuple  $(s, a, r, s')$  of state  $s$ , action  $a$ , the reward  $r = R(s, a)$  and the transition state  $s'$  collected from a demonstrator’s policy. In most cases these demonstrations are from a human observer, although in principle these demonstrations can come from any existing policy.

## Related Work

Several works have shown the efficacy of combining behavior cloning with reinforcement learning across a variety of tasks. Recent work by (Hester et al. 2018) combined behavior cloning with deep Q-learning (Mnih et al. 2015) to learn policies for Atari games by leveraging a loss function that combines a large-margin supervised learning loss function, 1-step Q-learning loss, and an  $n$ -step Q-learning loss function that helps ensure the network satisfies the Bellman equation. This work was extended to continuous action spaces by (Večerík et al. 2017), who proposed an extension of DDPG (Lillicrap et al. 2015) that uses human demonstrations, and applied their approach to object manipulation tasks for both simulated and real robotic environments. The loss functions for these methods include the  $n$ -step Q-learning loss, which is known to require on-policy data to accurately estimate. Similar work by (Nair et al. 2018) combined behavior cloning-based demonstration learning, goal-based reinforcement learning, and DDPG for robotic manipulation of objects in a simulated environment.

A method that is very similar to ours is the Demo-Augmented Policy Gradient (DAPG) (Rajeswaran et al. 2018), an approach that uses behavior cloning as a pre-training step together with an augmented loss function with a heuristic weight function, which interpolates between the policy gradient loss, computed using the Natural Policy Gradient (Kakade 2001), and behavior cloning loss. They apply their approach across four different robotic manipulations tasks using a 24 Degree-of-Freedom (DoF) robotic hand in a simulator and show that DAPG outperforms DDPGfD across all tasks. Their work also showed that behavior cloning combined with Natural Policy Gradient performed very similarly to DAPG for three of the four tasks considered, showcasing the importance of using a behavior cloning loss both in pre-training and policy training.

## Integrating Behavior Cloning and Reinforcement Learning

The Cycle-of-Learning (CoL) framework is a method for transitioning behavior cloning policies to RL by utilizing an actor-critic architecture with a combined BC+RL loss function and pre-training phase for continuous state-action spaces, in dense- and sparse-reward environments. The main advantage of using off-policy methods is to re-use previous data to train the agent and reduce the amount of interactions between agent and environment, which is relevant to robotic applications or real-world system where interactions can be costly.

The combined loss function consists of the following components: an expert behavior cloning loss that bounds actor’s action to previous human trajectories, 1-step return Q-learning loss to propagate values of human trajectories to previous states, the actor loss, and a  $L_2$  regularization loss on the actor and critic to stabilize performance and prevent over-fitting during training. The implementation of each loss component and their combination are defined as follows:

- **Expert behavior cloning loss ( $\mathcal{L}_{BC}$ ):** Given expert demonstration subset  $\mathcal{D}_E$  of continuous states and actions visited during a task demonstration over  $T$  time steps

$$\mathcal{D}_E = \{s_{E_0}, a_{E_0}, s_{E_1}, a_{E_1}, \dots, s_{E_T}, a_{E_T}\}, \quad (1)$$

a behavior cloning loss (mean squared error) from demonstration data  $\mathcal{L}_{BC}$  can be written as

$$\mathcal{L}_{BC}(\theta_\pi) = \frac{1}{2} (\pi(s_t|\theta_\pi) - a_{E_t})^2 \quad (2)$$

in order to minimize the difference between the actions predicted by the actor network  $\pi(s_t)$ , parametrized by  $\theta_\pi$ , and the expert actions  $a_{E_t}$  for a given state vector  $s_t$ .

- **1-step return Q-learning loss ( $\mathcal{L}_1$ ):** The 1-step return  $R_1$  can be written in terms of the critic network  $Q$ , parametrized by  $\theta_Q$ , as

$$R_1 = r + \gamma Q(s_{t+1}, \pi(s_{t+1}|\theta_\pi)|\theta_Q). \quad (3)$$

In order to satisfy the Bellman equation, we minimize the difference between the predicted Q-value and the observed return from the 1-step roll-out:

$$\mathcal{L}_{Q_1}(\theta_Q) = \frac{1}{2} (R_1 - Q(s_t, \pi(s_t|\theta_\pi)|\theta_Q))^2. \quad (4)$$

- **Actor Q-loss ( $\mathcal{L}_A$ ):** It is assumed that the critic function  $Q$  is differentiable with respect to the action. Since we want to maximize the Q-values for the current state, the actor loss became the negative of the Q-values predicted by the critic:

$$\mathcal{L}_A(\theta_\pi) = -Q(s, \pi(s|\theta_\pi)|\theta_Q). \quad (5)$$

Combining the above loss functions for the Cycle-of-Learning becomes

$$\begin{aligned} \mathcal{L}_{CoL}(\theta_Q, \theta_\pi) &= \lambda_{BC} \mathcal{L}_{BC}(\theta_\pi) + \lambda_A \mathcal{L}_A(\theta_\pi) \\ &+ \lambda_{Q_1} \mathcal{L}_{Q_1}(\theta_Q) + \lambda_{L_2} \mathcal{L}_{L_2}(\theta_Q) + \lambda_{L_2} \mathcal{L}_{L_2}(\theta_\pi). \end{aligned} \quad (6)$$

Our approach starts by collecting contiguous trajectories from expert policies and stores the current and subsequent state-actions pairs, reward received, and task completion signal in a permanent expert memory buffer  $\mathcal{D}_E$ . During the pre-training phase, the agent samples a batch of trajectories from the expert memory buffer  $\mathcal{D}_E$  containing expert trajectories to perform updates on the actor and critic networks using the same combined loss function (Equations 6). This procedure shapes the actor and critic initial distributions to be closer to the expert trajectories and eases the transition from policies learned through expert demonstration to reinforcement learning.

After the pre-training phase, the policy is allowed to roll-out and collect its first on-policy samples, which are stored in a separate first-in-first-out memory buffer with only the agent’s samples. After collecting a given number of on-policy samples, the agent samples a batch of trajectories comprising 25% of samples from the expert memory buffer and 75% from the agent’s memory buffer. This fixed ratio guarantees that each gradient update is grounded by expert trajectories. If a human demonstrator is used, they can intervene at any time the agent is executing their policy, and add this new trajectories to the expert memory buffer.

The proposed method is shown in Algorithm 1.

## Experimental Setup and Results

### Experimental Setup

As described in the previous sections, in our approach, the Cycle-of-Learning (CoL), we collect contiguous trajectories from expert policies and store them in a permanent memory buffer. The policy is allowed to roll-out and is trained with a combined loss from a mix of demonstration and agent data, stored in a separate first-in-first-out buffer. We validate our approach in three environments with continuous observation- and action-space: LunarLanderContinuous-v2 (Brockman et al. 2016) (dense and sparse reward cases) and a custom quadrotor landing task (Goecks et al. 2019) implemented using Microsoft AirSim (Shah et al. 2017). The dense reward case of LunarLanderContinuous-v2 is the standard environment provided by OpenAI Gym library (Brockman et al. 2016): state space consists of a eight-dimensional continuous vector with inertial states of the lander, action space consists of a two-dimensional continuous vector controlling main and side thrusts, and reward is given at every step based on the relative motion of the lander with respect to the landing pad (bonus reward is given when the landing is completed successfully). The sparse reward case is a custom modification with the same reward scheme and state-action space, however the reward is stored during the policy roll-out and is only given to the agent if the episode is over, zero otherwise. The custom quadrotor landing task is a modified version of the environment proposed by Goecks et al., implemented using Microsoft AirSim (Shah et al. 2017), which consists of landing a quadrotor on a static landing pad in a simulated gusty environment, as seen in Figure 1. The state space consists of a fifteen-dimensional continuous vector with inertial states of the quadrotor and visual features that represent the landing pad image-frame position and ra-

---

**Algorithm 1** Cycle-of-Learning (CoL): Transitioning from Demonstration to Reinforcement Learning
 

---

- 1: **Input:**  
 Environment  $env$ , number of training steps  $T$ , number of training steps per batch  $M$ , number of pre-training steps  $L$ , number of gradient updates  $K$ , and CoL hyperparameters  $\lambda_{Q1}$ ,  $\lambda_{BC}$ ,  $\lambda_A$ ,  $\lambda_{L2}$ ,  $\tau$ .
- 2: **Output:**  
 Trained actor  $\pi(s|\theta_\pi)$  and critic  $Q(s, \pi|\theta_Q)$  networks.
- 3: **Randomly initialize:**  
 Actor network  $\pi(s|\theta_\pi)$  and its target  $\pi'(s|\theta_{\pi'})$ .  
 Critic network  $Q(s, \pi|\theta_Q)$  and its target  $Q'(s, \pi'|\theta_{Q'})$ .
- 4: Initialize agent and expert replay buffers  $\mathcal{R}$  and  $\mathcal{R}_E$ .
- 5: Load  $\mathcal{R}$  and  $\mathcal{R}_E$  with expert dataset  $\mathcal{D}_E$ .
- 6: **for** pre-training steps = 1, ...,  $L$  **do**
- 7:   Call  $TrainUpdate()$  procedure.
- 8: **for** training steps = 1, ...,  $T$  **do**
- 9:   Reset  $env$  and receive initial state  $s_0$ .
- 10:   **for** batch steps = 1, ...,  $M$  **do**
- 11:     Select action  $a_t = \pi(s_t|\theta_\pi)$  according to policy.
- 12:     Perform action  $a_t$  and observe reward  $r_t$  and next state  $s_{t+1}$ .
- 13:     Store transition  $(s_t, a_t, r_t, s_{t+1})$  in  $\mathcal{R}$ .
- 14:     **for** update steps = 1, ...,  $K$  **do**
- 15:       Reset  $env$  and receive initial state  $s_0$ .
- 16:       **for** training steps  $t = 1, \dots, T$  **do**
- 17:         Call  $TrainUpdate()$  procedure.
- 18: **procedure** TRAINUPDATE()  
 19:   **if** Pre-training **then**  
 20:     Randomly sample  $N$  transitions  $(s_i, a_i, r_i, s_{i+1})$  from the expert replay buffer  $\mathcal{R}_E$ .  
 21:   **else**  
 22:     Randomly sample  $N * 0.25$  transitions  $(s_i, a_i, r_i, s_{i+1})$  from the expert replay buffer  $\mathcal{R}_E$  and  $N * 0.75$  transitions from the agent replay buffer  $\mathcal{R}$ .  
 23:     Compute  $\mathcal{L}_{Q1}(\theta_Q)$ ,  $\mathcal{L}_{BC}(\theta_\pi)$ ,  $\mathcal{L}_A(\theta_\pi)$ ,  $\mathcal{L}_{L2}(\theta_Q)$ ,  $\mathcal{L}_{L2}(\theta_\pi)$   
 24:     Update actor and critic for  $K$  steps according to Equation 6.  
 25:     Update target networks:

$$\begin{aligned}\theta_{\pi'} &\leftarrow \tau\theta_\pi + (1 - \tau)\theta_{\pi'}, \\ \theta_{Q'} &\leftarrow \tau\theta_Q + (1 - \tau)\theta_{Q'}.\end{aligned}$$


---

dus as seen by a downward-facing camera. The action space is a four-dimensional continuous vector that sends velocity commands for throttle, roll, pitch, and yaw. Wind is modeled as noise applied directly to the actions commanded by the agent and follows a temporal-based, instead of distance-based, discrete wind gust model (Moorhouse and Woodcock 1980) with 65% probability of encountering a wind gust at each time step. This was done to induce additional stochasticity in the environment. The gust duration is uniformly sampled to last between one to three real time seconds and



Figure 1: Screenshot of AirSim environment and landing task. Inset image in lower right corner: downward-facing camera view used for extracting the position and radius of the landing pad, which is part of the state space.

can be imparted in any direction, with maximum velocity of half of what can be commanded by the agent along each axis. This task has a sparse-reward scheme (reward  $R$  is given at the end of the episode, and is zero otherwise) based on the relative distance  $r_{rel}$  between the quadrotor and the center of the landing pad at the final time step of the episode:

$$R = \frac{1}{1 + r_{rel}^2}.$$

The hyperparameters used in CoL for each environment are described in the Supplementary Material.

The baselines for our approach are Deep Deterministic Policy Gradient (DDPG) (Lillicrap et al. 2015; Silver et al. 2014), Deep Deterministic Policy Gradient from Demonstrations (DDPGfD) (Večerík et al. 2017), and behavior cloning (BC). For the DDPG baseline we used an open-source implementation by Stable Baselines (Hill et al. 2018). The hyperparameters used concur with the original DDPG publication (Lillicrap et al. 2015): actor and critic networks with 2 hidden layers with 400 and 300 units respectively, optimized using Adam (Kingma and Ba 2014) with learning rate of  $10^{-4}$  for the actor and  $10^{-3}$  for the critic, discount factor of  $\gamma = 0.99$ , trained with minibatch size of 64, and replay buffer size of  $10^6$ . Exploration noise was added to the action following an Ornstein-Uhlenbeck process (Uhlenbeck and Ornstein 1930) with mean of 0.15 and standard deviation of 0.2. The DDPGfD baseline followed the same implementation for the loss function used in our approach (Equations 6) with some modifications: removal of the behavior cloning loss by setting  $\lambda_{BC} = 0$ , inclusion of the  $n$ -step loss as

$$\mathcal{L}_{Q_n}(\theta_Q) = \frac{1}{2} (R_n - Q(s, \pi(s|\theta_\pi)|\theta_Q))^2,$$

where  $R_n$  is written as

$$\begin{aligned}R_n &= r_t + \gamma r_{t+1} + \dots + \gamma^{n-a} r_{t+n-1} \\ &\quad + \gamma^n Q(s_{t+n}, \pi(s_{t+n}|\theta_\pi)|\theta_Q), \\ &= \sum_{i=0}^{n-1} \gamma^i r_i + \gamma^n Q(s_{t+n}, \pi(s_{t+n}|\theta_\pi)|\theta_Q),\end{aligned}$$

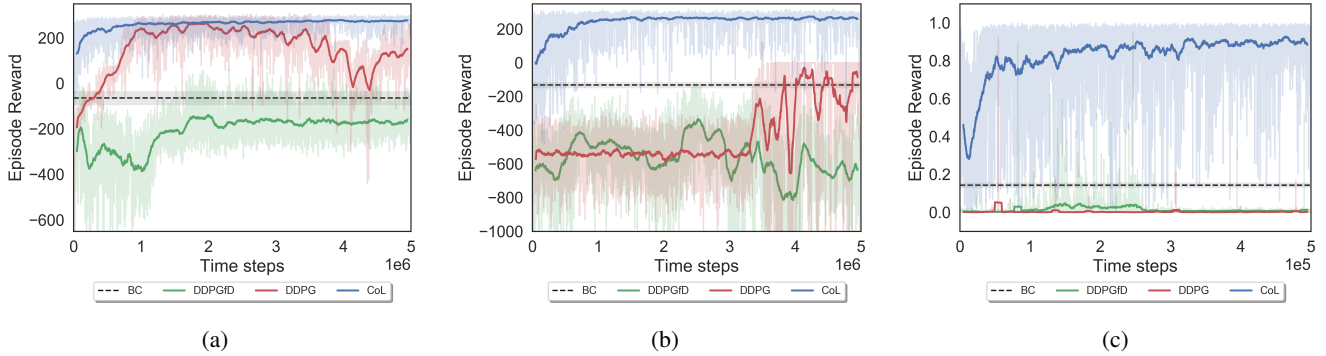


Figure 2: Comparison of CoL, BC, DDPG, and DDPGfD in the (a) dense- and (b) sparse-reward LunarLanderContinuous-v2 environment, and the (c) sparse-reward Microsoft AirSim quadrotor landing environment.

using  $n=10$ , following the Deep Q-learning from Demonstrations (DQfD) (Hester et al. 2018) implementation from which DDPGfD is derived, and using Prioritized Experience Replay (PER) (Schaul et al. 2015) to mix expert and agent samples instead of following a fixed ratio.

The BC policies are trained by minimizing the mean squared error between the expert demonstrations and the output of the model. The policies consist of a fully-connected neural network with 3 hidden layers with 128 units each and exponential linear unit (ELU) activation function (Clevert, Unterthiner, and Hochreiter 2015). The BC policy was evaluated for 100 episodes which was used to calculate the mean and standard error of the performance of the policy.

### Experimental results

The comparative performances of the CoL against the baseline methods (DDPG and DDPGfD) for the LunarLanderContinuous-v2 environment are presented via their training curves in Figure 2a, using the standard dense reward. The mean reward of the BC pre-trained from the human demonstrations is also shown for reference, and its standard error is shown by the shaded band. The CoL reward initializes to values at or above the BC and steadily improves throughout the reinforcement learning phase. Conversely, the DDPG RL baseline initially returns rewards lower than the BC and slowly improves until its performance reaches similar levels to the CoL after approximately one million steps. However, this baseline never performs as consistently as the CoL and eventually begins to diverge, losing much of its performance gains after about four million steps. The DDPGfD baseline performs even worse in this context, never consistently surpassing the BC performance.

When using sparse rewards, meaning only the rewards generated by the LunarLanderContinuous-v2 environment are provided only at the last time step of each episode, the performance improvement of the CoL relative to the DDPG and DDPGfD baselines is even greater (Figure 2b). The performance of the CoL is qualitatively similar during training to that of the dense case, with an initial reward roughly

equal to or greater than that of the BC and a consistently increasing reward. Conversely, the performance of the DDPG baseline is greatly diminished for the sparse reward case, yielding effectively no improvement for more than three million training steps before generating reward only comparable to the BC and the initial performance of the CoL. The training of the DDPGfD also deteriorates in this case, with even lower reward values and produces a more volatile, less stable training curve as is also seen for DDPG.

The results for the more realistic and challenging AirSim quadrotor landing environment (Figure 2c) illustrate a similar trend. The CoL initially returns rewards at or above the BC and steadily increases its performance, whereas the baseline approaches (DDPG and DDPGfD) practically never succeed and subsequently fail to learn a viable policy. Noting that successfully landing on the target would generate a sparse episode reward of approximately 0.64, it is clear that these baseline algorithms rarely generate a satisfactory trajectory for the duration of training.

### Ablation Studies

Several ablation studies were performed to evaluate the impact of each of the critical elements of the CoL on learning. These respectively include removal of the pre-training phase (*CoL-PT*), removal of the actor’s expert behavior cloning loss during pre-training and RL (*CoL-BC*), and use of standard behavior cloning and DDPG loss functions rather than the combined loss functions in Equations 6-6 (*BC+DDPG*). The results of each ablation condition are shown in Figure 3a and details about the ablation study can be found in Table 1.

*CoL-PT*: Cycle-of-Learning without the pre-training phase (number of pre-training steps  $L = 0$ ). The complete combined loss, as seen in Equations 6 is used during the reinforcement learning phase. This condition assesses the impact on learning performance of not pre-training the agent, while still using the combined loss in the RL phase. This condition differs from the baseline CoL in its initial performance being less, significantly below the BC, but does reach similar rewards after several hundred thousand steps, ex-

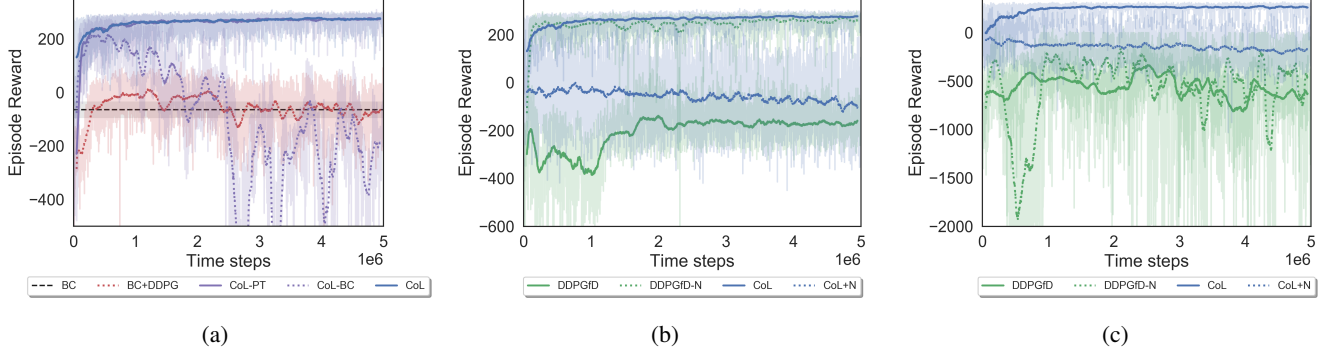


Figure 3: (a) Ablation study in LunarLanderContinuous-v2 environment comparing complete Cycle-of-Learning (CoL), CoL without the pre-training phase (CoL-PT), CoL without the expert behavior cloning loss (CoL-BC), and pre-training with BC followed by DDPG without combined loss (BC+DDPG). Comparison in LunarLanderContinuous-v2 environment for (b) dense and (c) sparse cases of the Cycle-of-Learning with (CoL+N) and without (CoL) the  $n$ -step loss, and DDPGfD with (DDPGfD) and without (DDPGfD-N) the  $n$ -step loss.

hibiting the same consistent response during training thereafter. Effectively, this highlights that the benefit of pre-training is improved initial response and some speed gain in reaching steady-state performance level, without qualitatively impacting the long-term training behavior.

**CoL-BC:** Cycle-of-Learning without the behavioral cloning expert loss on the actor ( $\lambda_{BC} := 0$ ) during both pre-training and RL phases. The critic loss remains the same as in Equation 6 for both training phases. This condition assesses the impact on learning performance of the behavior cloning loss component  $\mathcal{L}_{BC}$ , given otherwise consistent loss functions in both pre-training and RL phases. This condition improves upon the CoL-PT condition in its initial reward return and similarly achieves comparable performance to the baseline CoL in the first few hundred thousand steps, but then steadily deteriorates as training continues, with several catastrophic losses in performance. This result makes clear that the behavioral cloning loss is an essential component of the combined loss function toward maintaining performance throughout training, anchoring the learning to some previously demonstrated behaviors that are sufficiently proficient.

**BC+DDPG:** Behavior cloning with subsequent DDPG using standard loss functions (Equations 2, 4, and 5) rather than the CoL combined loss in both phases (Equation 6). Pre-training of the actor with behavioral cloning uses only the regression loss, as seen in Equation 2. DDPG utilizes standard loss functions for the actor and critic, as seen in Equation 7. This condition assesses the impact on learning performance of standardized loss functions rather than our combined loss functions across both training phases. This condition produces initial rewards similar to that of the CoL-PT condition, below the BC response. However, it subsequently improves in performance only to a level similar to that of the BC and is much less stable in its response throughout training. This result indicates that simply sequencing standard BC and RL algorithms results in both

poorer initial performance and a significantly lower level of performance and stability even after millions of training steps, emphasizing the value of a consistent combined loss function across all training phases.

$$\mathcal{L}_{DDPG}(\theta_Q, \theta_\pi) = \lambda_{Q_1} \mathcal{L}_{Q_1}(\theta_Q) + \lambda_A \mathcal{L}_A(\theta_\pi) + \lambda_{L_2} \mathcal{L}_{L_2}(\theta_Q) + \lambda_{L_2} \mathcal{L}_{L_2}(\theta_\pi). \quad (7)$$

### The $n$ -step Loss Contribution

In addition to the ablation study, we also investigated the effect of including an  $n$ -step Q-learning loss function in addition to the 1-step Q-learning loss function.  $n$ -step Q-learning has the advantage of faster convergence properties as the  $n$  previous Q-values are updated after receiving a reward, instead of only the next Q-value as is the case with 1-step Q-learning. This allows for faster propagation of the expected return to Q-values at earlier states and overall improves the efficiency of Q-learning. The downside of  $n$ -step Q-learning is that the Q-values are only actually correct when learning on-policy and thus off-policy techniques can generally not be used as in 1-step learning (Sutton et al. 1999).

To show the effect of the  $n$ -step Q-learning loss on the Cycle-of-Learning (CoL), we repeated experiments shown in Figures 2a and Figures 2b, for the dense and sparse reward cases in the LunarLanderContinuous-v2 environment, adding the  $n$ -step Q-learning loss ( $n=10$ ) (Hester et al. 2018)) to the combined loss function of the CoL, as well as removing this loss component from DDPGfD. The results for the dense and sparse case are shown in Figures 3b and 3c, respectively. For both dense and reward cases, the  $n$ -step Q-learning loss decreases the performance of the CoL, where it was not present originally, and its removal increases the performance of DDPGfD, where it was present originally. We believe this is because in order to learn accurate Q-values the  $n$ -step Q-learning loss needs to be applied to on-policy data, however, because each method is using a replay buffer of past data, the learning is actually off-policy.

Table 1: Method Comparison

Method	Plot Legend	Pre-Training Loss	Training Loss	Buffer Type	Average Reward
CoL	Blue, solid	$\mathcal{L}_{Q_1} + \mathcal{L}_A + \mathcal{L}_{BC}$	$\mathcal{L}_{Q_1} + \mathcal{L}_A + \mathcal{L}_{BC}$	Fixed Ratio	$261.80 \pm 22.53$
CoL-PT	Purple, solid	None	$\mathcal{L}_{Q_1} + \mathcal{L}_A + \mathcal{L}_{BC}$	Fixed Ratio	$253.24 \pm 46.50$
DDPGfD-N	Green, dash	None	$\mathcal{L}_{Q_1} + \mathcal{L}_A + \mathcal{L}_{BC}$	PER	$241.21 \pm 47.22$
DDPG	Red, solid	None	$\mathcal{L}_{Q_1} + \mathcal{L}_A$	Uniform	$152.98 \pm 69.45$
BC	Grey, solid	$\mathcal{L}_{BC}$	None	None	$-48.83 \pm 27.68^*$
BC+DDPG	Red, dash	$\mathcal{L}_{BC}$	$\mathcal{L}_{Q_1} + \mathcal{L}_A$	Uniform	$-57.38 \pm 50.11$
CoL+N	Blue, dash	$\mathcal{L}_{Q_1} + \mathcal{L}_{Q_n} + \mathcal{L}_A + \mathcal{L}_{BC}$	$\mathcal{L}_{Q_1} + \mathcal{L}_{Q_n} + \mathcal{L}_A + \mathcal{L}_{BC}$	Fixed Ratio	$-56.50 \pm 68.19$
CoL-BC	Purple, dash	$\mathcal{L}_{Q_1} + \mathcal{L}_A$	$\mathcal{L}_{Q_1} + \mathcal{L}_A$	Fixed Ratio	$-105.65 \pm 196.85$
DDPGfD	Green, solid	None	$\mathcal{L}_{Q_1} + \mathcal{L}_{Q_n} + \mathcal{L}_A + \mathcal{L}_{BC}$	PER	$-209.14 \pm 60.80$

Summary of learning methods. Enumerated for each method are all non-zero loss components (excluding regularization), buffer type, and average and standard error of the reward throughout training (after pre-training) across the three seeds, evaluated with dense reward in LunarLanderContinuous-v2 environment. \*For BC, these values are computed from 100 evaluation trajectories of the final pre-trained agent.

## Discussion and Conclusion

In this work, we present a novel method for combining behavior cloning with RL using an actor-critic architecture that implements a combined loss function and a demonstration-based pre-training phase. We compare our approach against state-of-the-art baselines, including BC, DDPG, and DDPGfD, and demonstrate the superiority of our method in terms of learning speed, stability, and performance with respect to these baselines. This is shown in the OpenAI Gym LunarLanderContinuous-v2 and the high-fidelity Microsoft AirSim quadrotor simulation environments. This result holds in both dense and sparse reward settings, though the improvements of our method over these baselines is even more dramatic in the sparse case. This result is especially noticeable in the AirSim landing task (Figure 2c), an environment designed to exhibit a high degree of stochasticity. The DDPG and DDPGfD baselines fail to learn an effective policy to perform the task, even after five million training steps, when using sparse rewards. Conversely, our method, CoL, is able to quickly achieve high performance without degradation, surpassing both behavior cloning and reinforcement learning algorithms alone, despite receiving only sparse rewards.

Additionally, we demonstrate through an ablation study of several components of our architecture that both pre-training and the use of a combined loss function are critical to the performance improvements. This ablation study also indicates that simply sequencing standard behavior cloning and reinforcement learning algorithms does not produce these gains. We also illustrate that the lack of a  $n$ -step Q-learning loss in our architecture is necessary for these improvements. Furthermore, we show that inclusion of such a loss term in our algorithm significantly reduces performance in both dense- and sparse-reward conditions, while its omission from DDPGfD significantly improves performance in dense-reward but not in sparse-reward conditions. To the best of our knowledge this is the first work that examined the effect of the  $n$ -step Q-learning loss on learning for DDPGfD policy performance.

Future work will investigate how to effectively integrate multiple forms of human feedback into an efficient human-in-the-loop RL system capable of rapidly adapting autonomous systems in dynamically changing environments. For example, existing works have shown the utility of leveraging human interventions (Goecks et al. 2019; Saunders et al. 2018), and specifically learning a predictive model of what actions to ignore at every time step (Zahavy et al. 2018). A limitation of our current approach is the requirement that the demonstrator be capable of generating a sufficient number of minimally proficient demonstrations, which can be prohibitive for humans in certain tasks with fast temporal dynamics or a high-dimensional action space. Deep reinforcement learning with human evaluative feedback has also been shown to quickly train policies across a variety of domains (Warnell et al. 2018; Arumugam et al. 2017) and can be a particularly useful approach when the human is unable to provide a demonstration of desired behavior but can articulate when desired behavior is achieved. Further, the capability our approach provides, to transition from a limited number of human demonstrations to a baseline behavior cloning agent and subsequent improvement through reinforcement learning without significant losses in performance, is largely motivated by the goal of human-in-the-loop learning on physical system. Thus our aim is to integrate this method onto such systems and demonstrate rapid, safe, and stable learning from limited human interaction.

## References

- [Andrychowicz et al. 2018] Andrychowicz, M.; Baker, B.; Chociej, M.; Jozefowicz, R.; McGrew, B.; Pachocki, J.; Petron, A.; Plappert, M.; Powell, G.; Ray, A.; et al. 2018. Learning dexterous in-hand manipulation. *arXiv preprint arXiv:1808.00177*.
- [Argall et al. 2009] Argall, B. D.; Chernova, S.; Veloso, M.; and Browning, B. 2009. A survey of robot learning from demonstration. *Robotics and autonomous systems* 57(5):469–483.

- [Arumugam et al. 2017] Arumugam, D.; Karamcheti, S.; Gopalan, N.; Wong, L. L. S.; and Tellex, S. 2017. Accurately and efficiently interpreting human-robot instructions of varying granularities. *CoRR* abs/1704.06616.
- [Brockman et al. 2016] Brockman, G.; Cheung, V.; Pettersson, L.; Schneider, J.; Schulman, J.; Tang, J.; and Zaremba, W. 2016. Openai gym. *arXiv preprint arXiv:1606.01540*.
- [Clevert, Unterthiner, and Hochreiter 2015] Clevert, D.-A.; Unterthiner, T.; and Hochreiter, S. 2015. Fast and accurate deep network learning by exponential linear units (elus). *arXiv preprint arXiv:1511.07289*.
- [Goecks et al. 2019] Goecks, V. G.; Gremillion, G. M.; Lawhern, V. J.; Valasek, J.; and Waytowich, N. R. 2019. Efficiently combining human demonstrations and interventions for safe training of autonomous systems in real-time. *AAAI Conference on Artificial Intelligence 33*.
- [Hester et al. 2018] Hester, T.; Vecerik, M.; Pietquin, O.; Lanctot, M.; Schaul, T.; Piot, B.; Horgan, D.; Quan, J.; Sendonaris, A.; Osband, I.; et al. 2018. Deep q-learning from demonstrations. In *Thirty-Second AAAI Conference on Artificial Intelligence*.
- [Hill et al. 2018] Hill, A.; Raffin, A.; Ernestus, M.; Gleave, A.; Traore, R.; Dhariwal, P.; Hesse, C.; Klimov, O.; Nichol, A.; Plappert, M.; Radford, A.; Schulman, J.; Sidor, S.; and Wu, Y. 2018. Stable baselines. <https://github.com/hill-a/stable-baselines>.
- [Kakade 2001] Kakade, S. 2001. A natural policy gradient. In *Proceedings of the 14th International Conference on Neural Information Processing Systems: Natural and Synthetic, NIPS'01*, 1531–1538. Cambridge, MA, USA: MIT Press.
- [Kingma and Ba 2014] Kingma, D. P., and Ba, J. 2014. Adam: A method for stochastic optimization. *arXiv preprint arXiv:1412.6980*.
- [Lillicrap et al. 2015] Lillicrap, T. P.; Hunt, J. J.; Pritzel, A.; Heess, N.; Erez, T.; Tassa, Y.; Silver, D.; and Wierstra, D. 2015. Continuous control with deep reinforcement learning. *arXiv preprint arXiv:1509.02971*.
- [Mnih et al. 2015] Mnih, V.; Kavukcuoglu, K.; Silver, D.; Rusu, A. a.; Veness, J.; Bellemare, M. G.; Graves, A.; Riedmiller, M.; Fidjeland, A. K.; Ostrovski, G.; Petersen, S.; Beattie, C.; Sadik, A.; Antonoglou, I.; King, H.; Kumaran, D.; Wierstra, D.; Legg, S.; and Hassabis, D. 2015. Human-level control through deep reinforcement learning. *Nature* 518(7540):529–533.
- [Moorhouse and Woodcock 1980] Moorhouse, D., and Woodcock, R. 1980. US Military Specification MIL-F-8785C. *US Department of Defense*.
- [Nair et al. 2018] Nair, A.; McGrew, B.; Andrychowicz, M.; Zaremba, W.; and Abbeel, P. 2018. Overcoming exploration in reinforcement learning with demonstrations. In *2018 IEEE International Conference on Robotics and Automation (ICRA)*, 6292–6299.
- [Rajeswaran et al. 2018] Rajeswaran, A.; Kumar, V.; Gupta, A.; Vezzani, G.; Schulman, J.; Todorov, E.; and Levine, S. 2018. Learning complex dexterous manipulation with deep reinforcement learning and demonstrations. In *Proceedings of Robotics: Science and Systems*.
- [Saunders et al. 2018] Saunders, W.; Sastry, G.; Stuhlmüller, A.; and Evans, O. 2018. Trial without error: Towards safe reinforcement learning via human intervention. In *Proceedings of the 17th International Conference on Autonomous Agents and MultiAgent Systems*, 2067–2069. International Foundation for Autonomous Agents and Multiagent Systems.
- [Schaul et al. 2015] Schaul, T.; Quan, J.; Antonoglou, I.; and Silver, D. 2015. Prioritized experience replay. *arXiv preprint arXiv:1511.05952*.
- [Shah et al. 2017] Shah, S.; Dey, D.; Lovett, C.; and Kapoor, A. 2017. Airsim: High-fidelity visual and physical simulation for autonomous vehicles. In *Field and Service Robotics*.
- [Silver et al. 2014] Silver, D.; Lever, G.; Heess, N.; Degris, T.; Wierstra, D.; and Riedmiller, M. 2014. Deterministic policy gradient algorithms.
- [Sutton and Barto 1998] Sutton, R., and Barto, A. 1998. *Reinforcement Learning: An Introduction*. MIT Press.
- [Sutton et al. 1999] Sutton, R. S.; Mcallester, D.; Singh, S.; and Mansour, Y. 1999. Policy Gradient Methods for Reinforcement Learning with Function Approximation. In *Advances in Neural Information Processing Systems 12* 1057–1063.
- [Uhlenbeck and Ornstein 1930] Uhlenbeck, G. E., and Ornstein, L. S. 1930. On the theory of the brownian motion. *Physical review* 36(5):823.
- [Večerík et al. 2017] Večerík, M.; Hester, T.; Scholz, J.; Wang, F.; Pietquin, O.; Piot, B.; Heess, N.; Rothörl, T.; Lampe, T.; and Riedmiller, M. 2017. Leveraging demonstrations for deep reinforcement learning on robotics problems with sparse rewards. *arXiv preprint arXiv:1707.08817*.
- [Warnell et al. 2018] Warnell, G.; Waytowich, N.; Lawhern, V.; and Stone, P. 2018. Deep tamer: Interactive agent shaping in high-dimensional state spaces. In *Thirty-Second AAAI Conference on Artificial Intelligence*.
- [Zahavy et al. 2018] Zahavy, T.; Haroush, M.; Merlis, N.; Mankowitz, D. J.; and Mannor, S. 2018. Learn what not to learn: Action elimination with deep reinforcement learning. In Bengio, S.; Wallach, H.; Larochelle, H.; Grauman, K.; Cesa-Bianchi, N.; and Garnett, R., eds., *Advances in Neural Information Processing Systems 31*. Curran Associates, Inc. 3562–3573.



## Supplementary Material

This supplementary material contains details of the implementation to improve reproducibility of the research work. Algorithm 1 describes all steps of the proposed method and Table 2 summarize all CoL hyperparameters used on the LunarLanderContinuous-v2 and Microsoft AirSim experiments.

Table 2: Cycle-of-Learning hyperparameters for each environment: (a) LunarLanderContinuous-v2 and (b) Microsoft AirSim.

Hyperparameter	Environments	
	(a)	(b)
$\lambda_{Q_1}$ factor	1.0	1.0
$\lambda_{BC}$ factor	1.0	1.0
$\lambda_A$ factor	1.0	1.0
$\lambda_{L_2}$ factor	$1.0e^{-5}$	$1.0e^{-5}$
Batch size	512	512
Actor learning rate	$1.0e^{-3}$	$1.0e^{-3}$
Critic learning rate	$1.0e^{-4}$	$1.0e^{-4}$
Memory size	$5.0e^5$	$5.0e^5$
Expert trajectories	20	10
Pre-training steps	$2.0e^4$	$2.0e^4$
Training steps	$5.0e^6$	$5.0e^5$
Discount factor $\gamma$	0.99	0.99
Hidden layers	3	3
Neurons per layer	128	128
Activation function	ELU	ELU